Cloud Feedback on SST Variability in the Western Equatorial Pacific in GOALS/LASG Model①

Liu Hui (刘 辉), *Zhang Xuehong* (张学洪) and *Wu Guoxiong* (吴国雄)
State Key Laboratory of Numerical Modeling for Atmospheric Sciences and Geophysical Fluid Dynamics (LASG), Institute of Atmospheric Physics (IAP), Chinese Academy of Sciences, P. O. Box 2718, Beijing 100080
Received October 30, 1997; revised December 11, 1997

ABSTRACT

The cloud feedback on the SST variability in the western equatorial Pacific in GOALS/LASG model is studied in this paper. Two versions of the model, one with the diagnostic cloud and another with the prescribed cloud, are used. Both versions are integrated for 45 years. It is found that in the prescribed cloud run, the SST variability in the western equatorial Pacific is mainly of interdecadal time scale and the interannual variability is very weak. In the diagnostic cloud run, however, the interdecadal SST variability is depressed much and the interannual SST variability becomes much significant.

The mechanism for the feedback is then explored. The variability of sea surface temperature (SST) in the western equatorial Pacific is found to be controlled mainly by the zonal wind anomaly, through the process of upwelling/downwelling in both versions. Then it is found that in the diagnostic cloud case, the negative feedback of the solar short wave (SW) flux acts significantly to balance the effect of upwelling/downwelling in addition to the latent flux. In addition, the variability of the SW flux is shown to be closely related to the variability of the middle and high cloud covers. Therefore, the negative feedback of the SW surface flux may have significant contribution to the cloud feedback on the SST variability.

Key words: Cloud feedback on SST variability

I. BACKGROUND

A global coupled ocean-atmosphere-land model (GOALS/LASG) has been established and developed in the LASG since 1994, which is composed of a nine-layer R15 AGCM and a $4^{o} \times 5^{o}$ twenty-layer global OGCM with a simple biosphere model included (see Wu et al., 1997 for its details). The ocean and atmosphere models are coupled with the monthly anomalies of heat flux and wind stress to reduce the impacts of systematic errors of each component model on the coupled system, where the anomaly is defined as the difference between the one of coupled run and the one of uncoupled climatology (Zhang et al., 1992; Yu and Zhang, 1997). In that version of the model, the cloud covers are prescribed monthly according to the climatology of International Satellite Cloud Climatology Project (ISCCP) cloud data and therefore there is no feedback from cloud.

It is found that in that version of the model the variability of sea surface temperature (SST) in the tropical region is not so reasonable. Fig. 1a shows the geographic distributions of the standard deviation of the SST. It can be seen that the variations of SST in the eastern

①This research is supported by the CNSF Projects No. 49475255, 49575265 as well as by the National Key Project Studies on Short-range Climate Prediction System of China, No. 96-908-04-03-3 and 96-908-02-03.

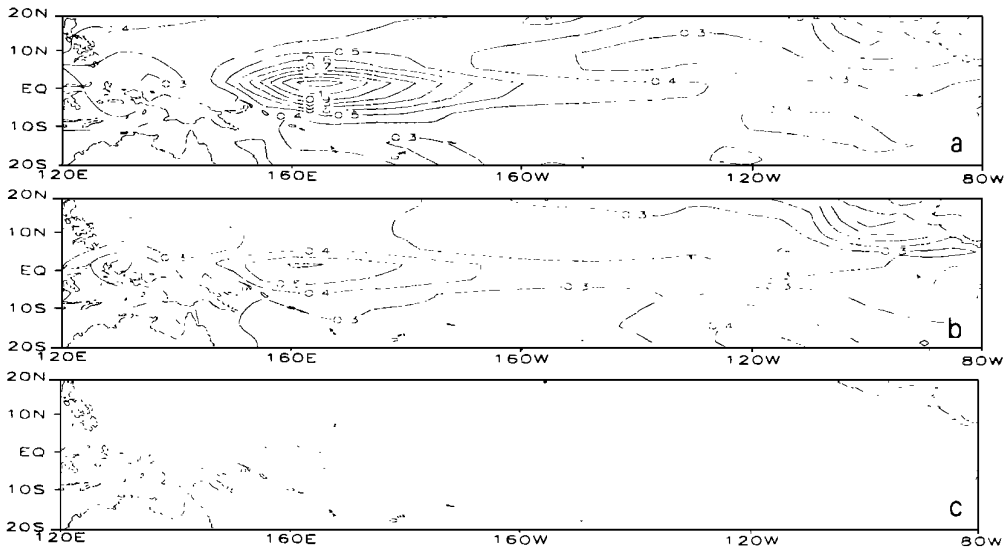

Fig. 1. Geographic distributions of the standard deviation of monthly mean SST from (a) prescribed cloud, (b) diagnosed cloud integration and (c) the difference between the prescribed and diagnosed cloud run. Unit: K.

equatorial Pacific is weak, only about 0.4°C; however, in the western equatorial Pacific, there is a very strong maximum of SST variation near 165°E, up to 1.1°C. This pattern of the variation is obviously not reasonable. One cause may be due to the lack of cloud feedback in this version of the model. Therefore, we would like to know whether the inclusion of cloud feedback may reduce significantly the SST variation in the western equatorial Pacific and further, if possible, increase the SST variation in the eastern Pacific.

A diagnosed cloud scheme is then developed and implemented into the model. In the following, the diagnosed cloud scheme will be presented firstly and then its simulation is compared with the ISCCP cloud data. The cloud feedback on the SST variations and the mechanism for the feedback will be explored. This is done mainly by comparing the results from the two versions of the model, that is, one with the prescribed cloud cover and another with the diagnosed cloud.

In this paper, only the effect of water cloud is considered in the model, that is, the effect of cirrus is not included yet.

II. DIAGNOSED CLOUD SCHEME AND ITS VALIDATION

1. *The Scheme*

Of the conditions required for the cloud formation, the relative humidity is believed to be the most important factor (Smagorinsky, 1960). For the marine stratus clouds, the temperature inversion may be another crucial one (Slingo, 1980). Therefore, the diagnosed cloud scheme used in the model is based on the relative humidity and temperature inversion.

The basic principles of the scheme are as follows:

The relative humidity is considered as the principal factor in evaluating cloud cover. Cloud is not distinguished into convective and non-convective ones.

Considering the previous observational and model studies (Slingo, 1980, 1987; Xu and Krueger, 1991), we choose a quadratic formula to diagnose the cloud cover from the relative humidity.

The thresholds of relative humidity at each layer are based on the suggestion of Xu and Krueger (1991). These values increase from the upper to lower part of the troposphere and the values are adjusted to get a best simulated total cloud cover, especially in the tropical region. At the moment, no cloud is allowed to form in the highest two model layers 1, 2 and the lowest model layer 9, that is, $\sigma = 0.0089$, $\sigma = 0.074$ and $\sigma = 0.991$ respectively.

The effect of vertical velocity is included, that is, no cloud is allowed to exist under strong subsidence.

The low marine stratus cloud associated with trade wind inversion is included because of its importance in air-sea interaction. We take the scheme of Slingo (1980) to parameterize it, mainly considering the simulated strength of the inversion in our model.

For the cloud water path (CWP), here we parameterize it in terms of the form of decay exponentially with height, as used in CCM3. This formula roughly represents the real situation.

The following are the procedures for evaluating the cloud cover and water path:

a) Cloud cover, A_1, under the condition of $RH > RH_C$

$$RH_C(\sigma) = \begin{cases} 0.60 & \sigma = \sigma_3,\ \sigma_4 \\ 0.78 & \sigma = \sigma_5,\ \sigma_6 \\ 0.85 & \sigma = \sigma_7,\ \sigma_8 \end{cases} \tag{1}$$

$$A_1 = \begin{cases} \left(\dfrac{RH - RH_C(\sigma)}{1 - RH_C(\sigma)}\right)^2 & \omega < 0 \\ \dfrac{\omega_C - \omega}{\omega_C}\left(\dfrac{RH - RH_C(\sigma)}{1 - RH_C(\sigma)}\right)^2 & 0 \leqslant \omega \leqslant \omega_C \\ 0 & \omega > \omega_C \end{cases} \tag{2}$$

where ω_C is chosen as 50 hPa/day, and σ_i is the sigma value of each layer, with the index i starting from the top.

b) Low marine stratus cloud, A_2, under the inversion condition (only over ocean)

Inversion condition:

$$\left(\frac{\partial\theta}{\partial p}\right)_{\min} = \min\left\{\left(\frac{\partial\theta}{\partial p}\right)_{\sigma_7}, \left(\frac{\partial\theta}{\partial p}\right)_{\sigma_8}\right\} \leqslant 0.07 \text{ K/hPa} \tag{3}$$

$$A_2 = \begin{cases} -16.67\left(\dfrac{\partial\theta}{\partial p}\right)_{\min} - 1.167 & RH_b > 0.8 \\ \left(-16.67\left(\dfrac{\partial\theta}{\partial p}\right)_{\min} - 1.167\right) \times \left(1 - \dfrac{0.8 - RH_b}{0.2}\right) & 0.6 \leqslant RH_b \leqslant 0.8 \\ 0 & RH_b < 0.6 \end{cases} \tag{4}$$

where RH_b is the relative humidity at the cloud base ($\sigma = \sigma_8$).

The combined low cloud covers ($\sigma = \sigma_7, \sigma_8$) are given by

$$A_L = \begin{cases} A_2 & \text{if } \left(\frac{\partial\theta}{\partial p}\right)_{\min} \leqslant -0.07 \text{ K/hPa} \\ A_1 & \text{otherwise} \end{cases} \tag{5}$$

c) Cloud Water Path is determined according to

$$CWP(k) = \int_{z_k}^{z_{k+1}} A \cdot \exp(-z/h_l)\, dz\,, \tag{6}$$

where $h_l = 700 \times \ln\left(1 + \int_{p_t}^{p_s} q \frac{dp}{g}\right)$, and the parameter A is specified as $0.05\ \mathrm{gm}^{-3}$, which is selected based on the data of SSM/I and GRODY (Chen et al., 1996).

The type of cloud is assigned roughly according to heights, that is:

Altostratus (As)	$\sigma = \sigma_3, \sigma_4$
Stratus (St)	$\sigma = \sigma_5, \sigma_6$
Cumulus (Cu)	$\sigma = \sigma_7, \sigma_8$

(7)

The cirrus does not exist in the model and so it is not considered in the high cloud.

For the purpose of diagnosis, the total cloud cover is calculated by assuming that cloud is random overlapped in all the vertical layers in which there are clouds. On the other hand, the overlapping of high, middle, and low clouds is calculated for the highest, middle, and lowest two layers respectively.

2. *Validation*

In the following, the cloud cover and outgoing long wave radiation (OLR) simulated from an Atmospheric Model Intercomparison Project (AMIP) run of the AGCM component are compared with observational data. Fig. 2 shows the simulated zonally averaged total cloud cover fraction for January and July, averaged for the ten AMIP years (1979–1988) and the corresponding ones from ISCCP data. It can be seen that the peak values within the tropical region for both months are captured. The model also simulates the peak values at both

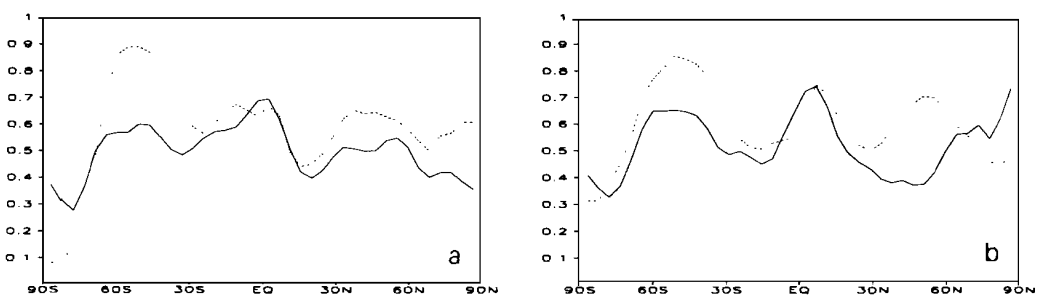

Fig. 2. Zonal-mean total cloud cover fraction of the AMIP run and ISCCP data for (a) January and (b) July. The dashed line is for ISCCP data.

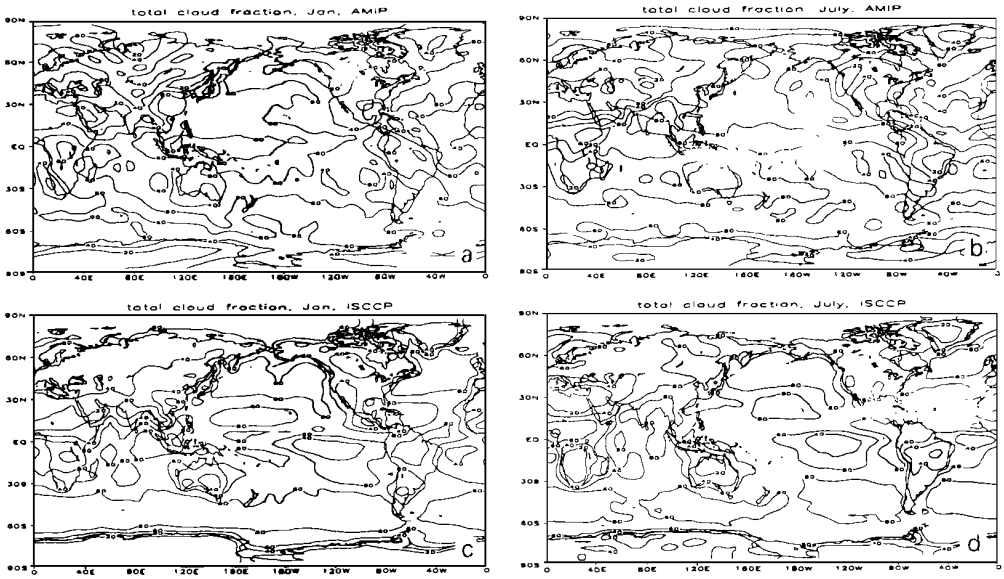

Fig. 3. The global distribution of total cloud cover fraction of the AMIP run for (a) January and (b) July, averaged for the ten years. (c) January and (d) July climatology of ISCCP. Unit: percentage (%), contour interval: 20.

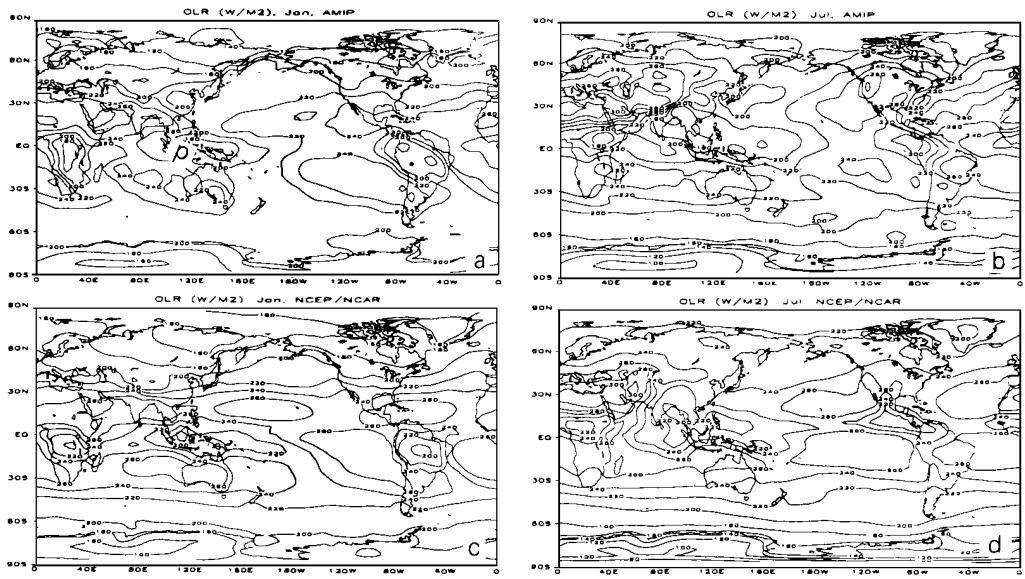

Fig. 4. (a) January and (b) July mean global distribution of outgoing long wave radiation (OLR) of the AMIP run and (c) January and (d) July mean OLR from the NCEP/NCAR reanalyses for 1979–1988. Unit: W/m^2.

hemispheric midlatitudes during the winter time, which is related to the storm-track, although they are underestimated somewhat compared to the observation. During the summer time, however, the simulated cloud cover at the northern mid-latitudes is out of phase with the observed one. It should be pointed out that in the ISCCP data, the cloud cover at midlatitudes of the two hemispheres may be overestimated, in contrast to other data sets, e.g., NIMBUS-7 data (Stowe et al., 1989).

The geographic distribution of total cloud cover fraction is given in Fig. 3. A major point is that the zonal pattern over the tropical region is simulated reasonably in both January and July. The major high values over the warm pool of the western Pacific, off the coast of Somali, central Africa and northern South America as well as the low value over the eastern Pacific are all well simulated. In July, the northward extension of cloud cover over Southeast Asia is simulated reasonably.

The simulated OLR is compared with the corresponding one determined from NCEP/NCAR reanalysis in Fig. 4. It can be seen that the patterns of shaded (maximum) and unshaded (minimum) regions are basically in agreement between the model and the observation. The northward extension of low OLR over India, southeastern Asia and the western Pacific is also reasonably simulated in July.

Therefore, the diagnosed cloud scheme can simulate basically the main characteristics of cloud in the observational data, especially in the tropical region.

III. CLOUD FEEDBACK ON SST ANOMALY

The geographic distributions of the standard deviation of the SST anomaly for the diagnostic cloud (DC) integration is shown in Fig. 1b. A significant fact is that the maximum of SST variation near 165°E is reduced evidently, now only up to 0.6°C. Therefore, the introducing of diagnostic cloud indeed has strong "negative feedback" on the amplitude of SST variability in the western Pacific. On the other hand, the cloud does not have significant impact on the SST variation in the eastern Pacific.

To get more details of this feedback, the SST anomaly averaged over the western equatorial Pacific region of 157.5—172.5°E, 4°N—4°S, where the standard deviation of SST reaches its maximum, is shown in Figs. 5a and 5b for the two runs. Here, the "anomaly" is defined as the deviation from the monthly mean climatology obtained from the average of the 45 year integration. It can be seen that in addition to the much depressed amplitude of SST variability in the DC case, another interesting point is that the variation of the SST anomaly is moved onto much shorter time-scale in the DC case compared with the PC case. From the power spectra of the SST anomalies (Figs. 5c and 5d), it can be clearly seen that the SST variability is mainly of interdecadal time scale of the periods of 7 and 20 years in the PC case. There is almost no significant interannual variability of SST. This is not realistic because the interannual variability is dominant there in the observations. In the DC case, however, the situation is quite different. It can be seen that the spectral power density with the interdecadal time scale is much reduced. In other words, the SST anomaly is much decreased on the interdecadal time scale. On the other hand, the SST anomaly becomes now much significant on the interannual time scale, e.g., the period of 3 years. The spectral power density at that period is up to 8%.

The above results demonstrate clearly that the feedback of cloud can greatly reduce the interdecadal variability of SST and greatly increase the interannual variability over the western equatorial Pacific region.

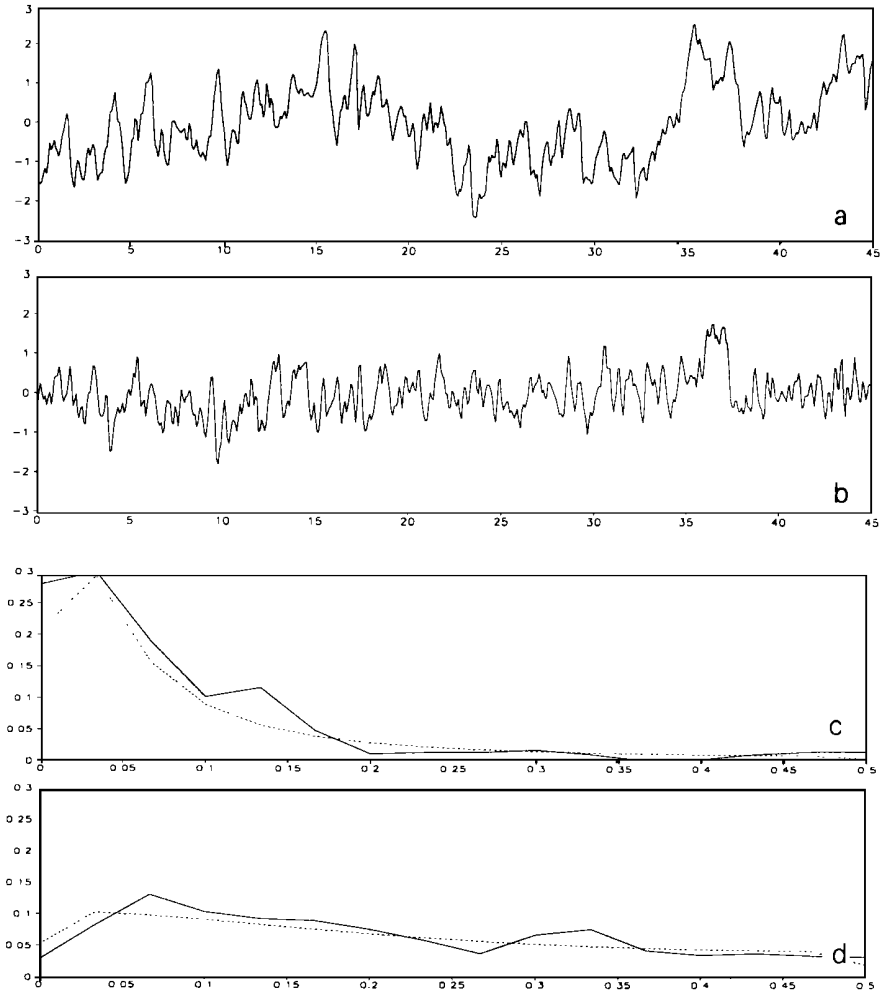

Fig. 5. Time evolution of SST anomaly averaged over the region of 157.5—172.5°E, 4°N—4°S for the 45 years for (a) prescribed and (b) diagnostic cloud run. Unit: K. The power spectra for (a) and (b) are shown in (c) and (d) respectively. The vertical coordinate in (c) and (d) is the spectral power density and the dashed line is the corresponding spectrum of red noise.

IV. EXPLANATION FOR THE FEEDBACK

1. *Discussion of Heat Balance at Sea Surface*

A question is what mechanism is responsible for the cloud feedback on variability of SST. According to the heat balance equation for SST, the related factors are: advection by currents, upwelling/downwelling in ocean, latent and sensible heat fluxes at surface, net short- and long- wave radiation fluxes at sea surface, as well as vertical diffusion.

a) Current advection and upwelling/downwelling

The current advection associated with westerly wind anomaly in the western equatorial Pacific can be found in most observed El Nino events and the westerly wind anomaly accompanies the SST anomaly (Cao, 1993). The effect of advection by currents is found to be

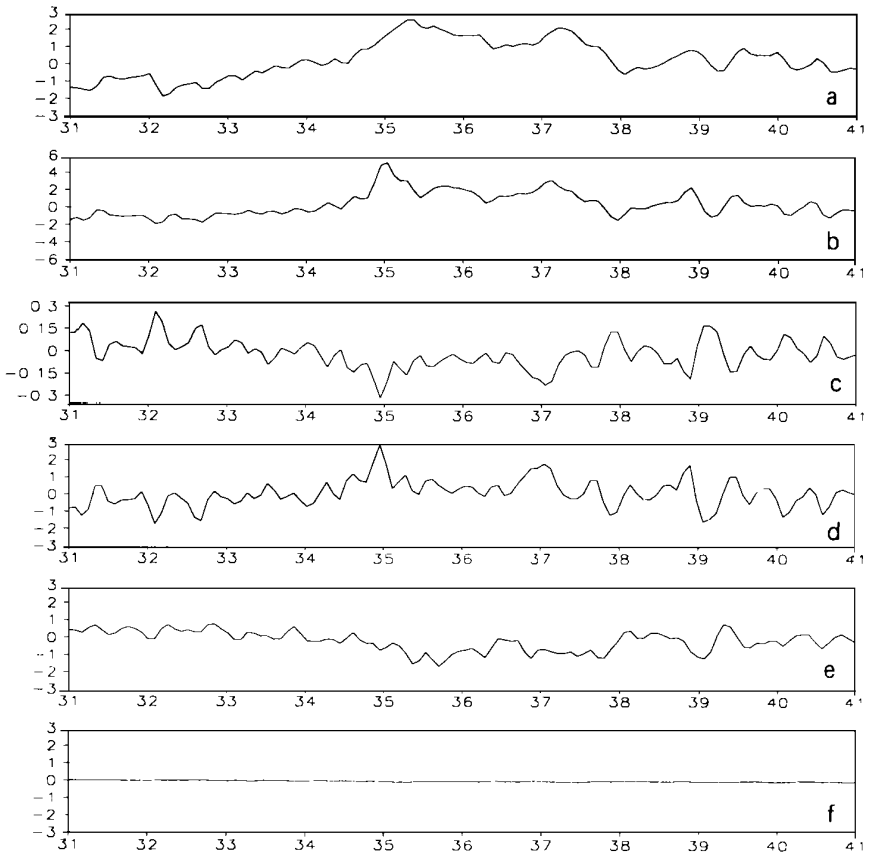

Fig. 6. Time evolution of anomaly of (a) SST, (b) zonal wind and (c) vertical velocity at the interface between the top layer and second layer in ocean, the tendencies of SST due to (d) upwelling/downwelling, (e) latent heat flux and (f) net SW flux for the prescribed cloud run over the region of 157.5—172.5°E, 4°N—4°S. Units: wind: m_s; vertical velocity: m/day, positive for upward; all tendencies: 0.01 K/day; latent heat flux: positive for upward.

comparable with the latent heat flux and short-wave radiation flux in the upper ocean heat budget from observation (Cronin et al., 1997). In the current CGCM, however, the contribution from the current advection is much smaller than that from the upwelling/downwelling in the surface layer of ocean in the western Pacific near the equator (not shown). This is, of course, a systematic bias of the model.

b) Latent and sensible heat flux.

The latent heat flux is a major way to extract water vapor and heat from the ocean into atmosphere and it is also important for the variability of SST. Increase of latent heat flux may also cause increase of cloud amount. However, impacts of cloud on the latent heat flux seem not as direct as on the SW flux and may be more complex. For the sensible heat flux, many observational and modeling studies demonstrate that it is much smaller than the latent heat flux and can be neglected over the equatorial oceans.

c) Surface Short wave (SW) and Long wave(LW) flux.

The SW flux arrived at surface is strongly influenced by clouds. Cloud can reflect most part of incident SW flux. On the other hand, however, cloud's impact on the net LW flux at

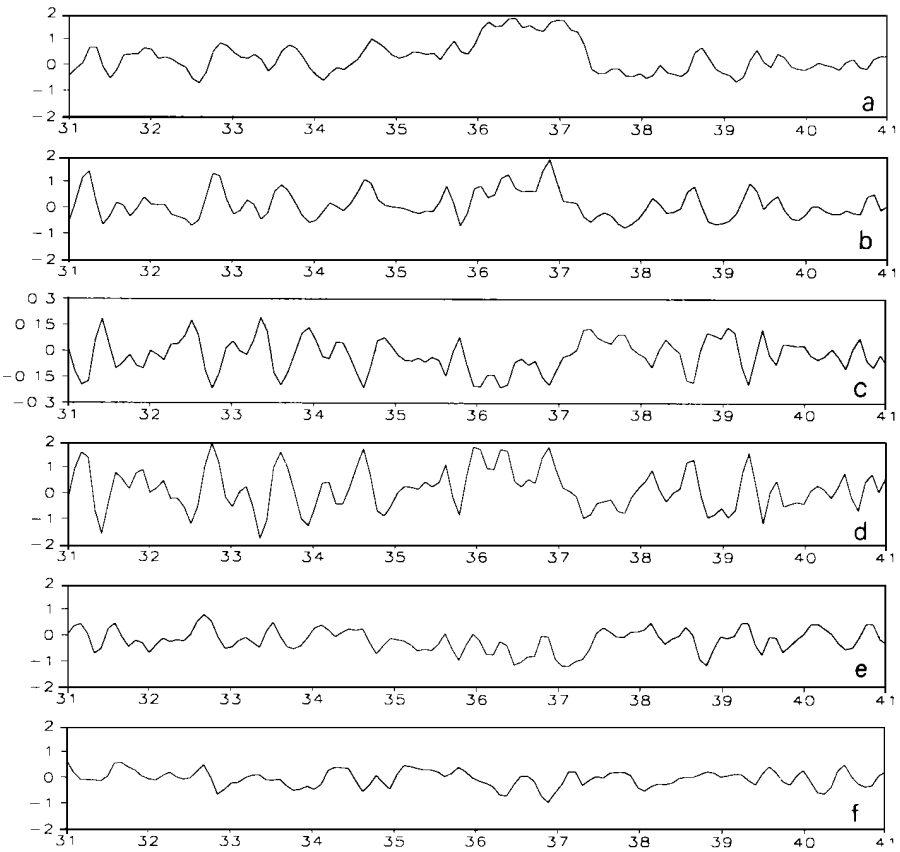

Fig. 7. Same as Fig. 6 except for the diagnostic cloud run.

surface is much weaker than the SW flux in the western Pacific in the model. It is found that the variability of net LW flux at surface is about 5 W/ m^2, only about 1_3 of SW flux at surface (not shown). This has been confirmed by some observations, e.g., Cronin et al. (1997).

Therefore, the upwelling/downwelling, latent heat flux, and SW flux are the most important factors to the SST tendency in the model. In the following, we will mainly focus on the mechanism of SW flux feedback on the SST tendency.

2. *Prescribed Cloud Case*

Fig. 6 shows the time– evolution of the anomalies of (a) SST, (b) zonal wind and (c) vertical velocity at the interface between the top layer and the second layer in ocean, the cooling/heating rates due to (d) upwelling/downwelling, (e) latent heat flux and (f) net SW flux over the same region as in Fig. 5. For a better display, only the years 32– 41 are shown here. We take the period of the years 34– 38 for discussions, which is a warm episode. It can be seen that during the period, the wind anomaly goes to westerly. As the wind anomaly goes to westerly, the vertical velocity anomaly becomes negative, that is, downward increased correspondingly. This in turn tends to increase the SST.

On the other hand, the latent heat flux tends to offset the effect of downwelling with a lag of a few months. It can be seen that this is the only negative feedback to the effect of downwelling due to lack of feedback from the SW flux. In this case, the warm episode lasts

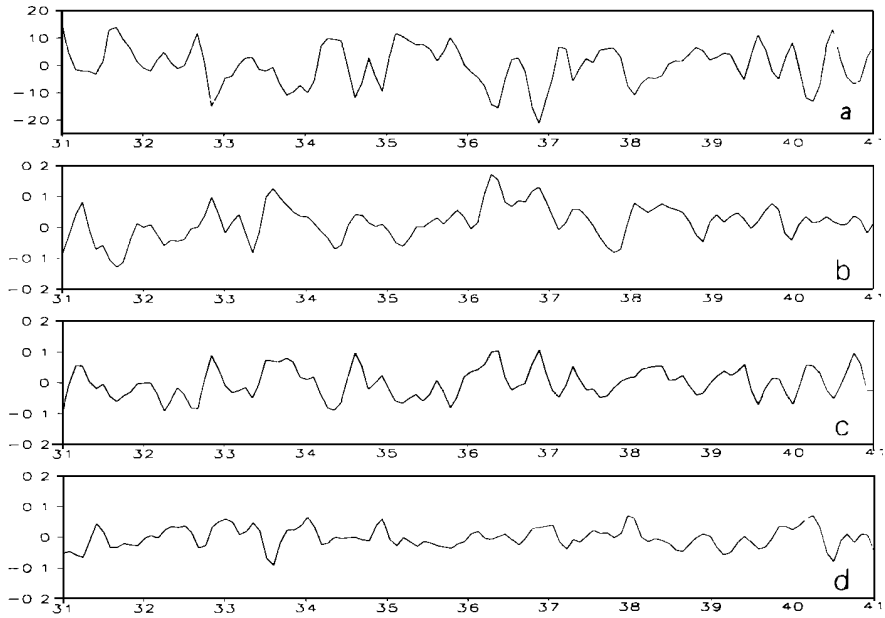

Fig. 8. Time evolution of the regionally averaged anomaly of (a) net SW flux, (b) high, (c) middle, and (d) low cloud cover for the diagnostic cloud run. Unit: SW: W/m^2, positive for downward.

longer time, about 3 years.

3. *Interactive Cloud Case*

For the diagnostic case (Fig. 7), we take the period of years 36–37, when a strong warm event of SST occurs, as an example. Again it can be seen that the wind anomaly goes to westerly during the period. The vertical velocity anomaly is therefore negative, that is, downward increased. Correspondingly, the anomalous downwelling results in increasing of SST.

On the other hand, the heating rate due to latent heat also tends to offset the effect of downwelling again with a lag of a few months. The negative feedback from the SW flux is now significant and of comparable magnitude to the latent heat flux. This demonstrates that the feedback from the SW flux may be a very important factor for the cloud feedback on the SST variability.

To reveal the relation between the SW flux feedback and cloud variability, the time evolution of the regionally averaged anomaly of (a) SW flux, (b) high–, (c) middle–, and (d) low–cloud cover fraction is shown in Fig. 8. It can be seen that the SW flux has significant negative correlation with all of the three cloud covers. The highest correlation coefficient is –0.83 for the middle cloud. So, the SW flux variability is indeed closely related to the variability of cloud cover, especially the middle one.

4. *Discussion*

It can be seen by comparing Figs. 6 and 7 that the wind anomaly, upwelling/downwelling and latent heat flux all have corresponding changes due to the included cloud feedback, that is, their interannual variations are increased. However, it is difficult to tell whether these factors are also responsible for the cloud feedback on the SST variability due to the complexity

of the problem. Therefore, the surface SW feedback due to inclusion of cloud feedback may be only one of the important mechanisms for the cloud feedback on the SST variability.

The cloud feedback, however, may increase the variability of atmospheric circulation even without the feedback of SST. This may get some support of the following fact. The correlation coefficient between the SST anomaly and surface divergence/zonal wind anomaly of atmosphere is up to −0.53/+0.85 in the prescribed cloud situation, but it is reduced to only −0.34/+0.56 in the diagnostic cloud situation. That means that the relationship between SST and surface wind is much reduced in the DC case.

V. CONCLUSION

Two versions of the GOALS/LASG model, one with the prescribed cloud and another with the diagnosed cloud, are compared to study the cloud feedback on SST variability in the tropical area, especially on interannual/interdecadal time scale. It is found that in the prescribed cloud case, the SST variability of the western equatorial Pacific is mainly of interdecadal time scale. In the interactive cloud case, however, the amplitude of the interdecadal SST variability is depressed much and the interannual SST variability becomes much significant in this region. This suggests that cloud feedback can result in significant increase of interannual variability of SST there.

It is further explored that the variability of SST in the western equatorial Pacific is mainly controlled by the zonal wind anomaly, through the process of upwelling/downwelling. In the diagnosed cloud case, the SW flux acts significantly to balance the effect of upwelling/downwelling in addition to the latent flux. The variability of SW flux is closely related to the variability of cloud cover, especially the middle and high clouds.

Therefore, it may be concluded that the cloud feedback has significant impacts on the SST variability in the western equatorial Pacific at both interannual and interdecadal time scales, and the surface SW flux feedback has significant contribution to the cloud feedback.

REFERENCES

Cao, J. P. (1993), *ENSO Dynamics*, China Meteorological Press, 309 pp (in Chinese).

Chen C.-T., and E. Roeckner, 1996, Cloud simulation with the MPI GCM ECHAM4 and comparison with observation, MPI Report No. 193.

Cronin M. F., and M. J. McPhaden (1997), The upper ocean heat balance in the western equatorial Pacific warm pool during September–December 1992, *J. Geophys. Res.*, **102(c4)**: 8533–8553.

Liu H., X.-Z. Jin, X-.H. Zhang and G.-X. Wu (1996), A coupling experiment of an atmosphere and an ocean model with a monthly anomaly exchange scheme, *Advances in Atmospheric Sciences*, **13(2)**: 133–146.

Slingo, J. M. (1980), A cloud parameterization scheme derived from GATE data for use with a numerical model, *Quart. J. R. Met. Soc.*, **106**: 747–770.

Stowe, L. L., Yeh H. Y. M., T. F. Eck, C. G. Wellemeyer and H. L. Kyle (1989), Nimbus-7 global cloud climatology. Part II: First year results, *J. Climate*, **2**: 671–709.

Wu, G.-X., H. Liu, Y.-C. Zhao, and W.-P. Li(1996), A nine-layer atmospheric general circulation model and its performance, *Advances Atmospheric Sciences*, **13(1)**: 1–18.

Wu, G.-X., Zhang X.-H., Liu H., Yu Y.-Q., Jin X.-Z., Guo, Y.-F., Sun, S.-F., Li, W.-P., Wang B. and Shi G.-Y. (1997), Global Ocean–Atmosphere–Land system model of LASG (GOALS/LASG) and its performance in simulation study, *Quarter Journal of Applied Meteorology*, **Vol. 8, Suppl.**, 15–28 (in Chinese).

Xu, K-M. and S. K. Krueger (1991), Evaluation of cloudiness parameterizations using a cumulus ensemble model, *Mon. Wea. Rev.*, **119**: 342–367.

Yu, Y. – Q. and X. H. Zhang (1997), A modified air– sea flux anomaly coupling scheme (in Chinese), accepted by KEXUE TONGBAO.

Zhang, X. – H., N. Bao, R. – C. Yu, and W. – Q. Wang (1992), Coupling experiments based on an atmospheric and an oceanic GCM, *Chinese Journal of Atmospheric Sciences*, **16**: 129– 144.

Zhang X. – H., K. – M. Chen, X. – Z. Jin, W. – Y. Lin, and Y. – Q. Yu (1996), Simulation of thermohaline circulation with a twenty– layer oceanic general circulation model, *Theoretical and Applied Climatology*, **55**: 65– 88.